

KEK-TH-416  
KEK Preprint 94-127  
KOBET-TH-94-02

## A Natural Explanation of All Solar Neutrino Data by Resonant Spin-Flavor Precession Scenario

C. S. Lim and H. Nunokawa<sup>†</sup>

*Department of Physics, Kobe University, Nada, Kobe 657, Japan*  
*Theory Group, KEK, Oho, Tsukuba 305, Japan*<sup>†</sup>

### Abstract

It is emphasized that the  $E_\nu$  (neutrino energy) spectrum of the  $\nu_e$  survival probability in the Resonant Spin-Flavor Precession (RSFP) scenario has very desirable shape to reconcile all existing solar neutrino data. As the result, the RSFP scenario is shown to have rather broad allowed region to reconcile the data in the  $(B, \Delta m^2)$  plane, with  $B$  being the magnetic field strength inside the Sun. The sensitivity of the allowed region on the different choices of the  $B$  profile, and the time variations of the solar neutrino event rates in the RSFP scenario are also discussed in some detail.

October 1994

The solar neutrino problem seems to be almost unique remaining puzzle, which cannot be resolved by the standard model of particle interactions, and therefore requires some “new physics”. The most simple and elegant particle physics solution to this problem by Mikheyev, Smirnov, and Wolfenstein (MSW) [1] relies on the resonant enhancement of neutrino oscillations inside the medium of the Sun. Another attractive solution was proposed by Okun, Voloshin, and Vysotsky (OVV) [2], which originally aimed to explain not only the deficit of the solar neutrino event rates, but also the possible anticorrelation of the solar neutrino flux with the sunspot number, claimed to exist in the Cl (Homestake) experiment [3]. The scenario of OVV assumes that  $\nu_e$  possesses a “large” magnetic moment. The “large” magnetic moment, when coupled to the strong transverse magnetic field inside the Sun, leads to a spin precession  $\nu_{eL} \rightarrow \nu_{eR}$ , yielding a sterile state,  $\nu_{eR}$ , which escapes the detection. Once the interaction of  $\nu_{eL}$  with the solar matter is taken into account, however, the matter effect causes an energy gap between  $\nu_{eL}$  and  $\nu_{eR}$  and tends to prevent the spin precession. We should also notice that the extent of spin precession has nothing to do with the neutrino energy  $E_\nu$ . To account for all of the now available data on the three types of solar neutrino experiments, i.e. Cl (Homestake)[3, 4],  $\nu e$  (Kamiokande) [5, 6], and Ga (SAGE [7, 8] and GALLEX [9]) experiments, therefore seems to be a non-trivial task, since these experiments have sensitivities on different ranges of  $E_\nu$  and are reporting different  $\nu_e$  deficit rates.

These problems can be evaded in a natural manner in the scenario of Resonant Spin-Flavor Precession (RSFP for short) [10, 11]. The basic observation of the scenario is that the matter effect, which prevents the spin precession in the OVV scenario, now works to realize resonant enhancement of the spin-flavor precessions, e.g.  $\nu_{eL} \rightarrow \nu_{\mu R}$  for Dirac type precession,  $\nu_{eL} \rightarrow \bar{\nu}_{\mu R} (= (\nu_{\mu L})^C)$  for Majorana type precession. The deficit rate of  $\nu_e$  now has a  $E_\nu$  dependence. (In the Majorana case the spin precession  $\nu_{eL} \rightarrow \bar{\nu}_{eR}$  is forbidden by CPT and the spin-flavor precession via transition magnetic moment is an inevitable choice.) The Majorana type RSFP, which we will consider in this paper, has additional bonuses: i) In the Majorana type transition the final state neutrino, e.g.  $\bar{\nu}_{\mu R}$ , is no longer sterile and does have a contribution to the event rate at Kamiokande. This feature is desirable in trying to explain the higher event rate and the milder time-dependence of the rate at Kamiokande compared with those in Cl data [12]. ii) Since the antineutrinos are trapped in dense stars and since sterile neutrinos do not appear in the interaction due to the transition moment, the severe astrophysical constraint coming from SN1987A neutrino data [13] and the cosmological

constraint on the number of neutrino species  $N_\nu < 3.4$  [14] can be easily lifted.

Now that the data from all of the three types of solar neutrino experiments are available, the RSFP scenario is ready to be confronted with these data. In particular, the most recent data from the Ga experiments [7, 8, 9] show relatively high event rates, and the result has been argued to disfavor the RSFP, since it contradicts with the large depletion of the  $pp$  neutrinos predicted in the interesting works in Ref. [15], which tried to reconcile the Cl and  $\nu e$  results (before the appearance of the Ga data), paying attention to their different energy thresholds.

In this paper, however, the all different deficit rates of the three types of experiments are shown to be simultaneously explained in a natural manner in the framework of RSFP scenario. This controversy suggests that the large depletion of the  $pp$  neutrino is not a genuine feature of RSFP, but rather may be due to the choice of parameters in the theory. We thus feel it very important to make clear what is the genuine predictions of RSFP, and which kinds of properties depend upon the specific choices of the parameters, before we derive some definite conclusion on the validity of the scenario. In the present paper we therefore try to extract some generic prediction of RSFP and to confront it with the observations. As such a generic feature we focus on the specific  $E_\nu$  dependence of the survival probability of  $\nu_e$ ,  $P_\nu \equiv P(\nu_e \rightarrow \nu_e)$ , in RSFP.

We would like to emphasize that the  $E_\nu$  dependence of  $P_\nu$  in RSFP is exactly what we want in order to explain the different event rates in three types of experiments, and is quite different from the  $E_\nu$  dependence in MSW. Namely, as is seen in Fig. 1, which shows a generic  $E_\nu$  dependence in RSFP for suitable range of the transverse magnetic field  $B$ , the survival probability behaves as,  $P_\nu \sim 1$  for smaller  $E_\nu$ ,  $P_\nu \sim 0$  for intermediate  $E_\nu$ , and  $P_\nu \sim 1/2$  for higher  $E_\nu$ . This behavior is immediately realized to be very desirable to reconcile the reported averaged deficit rates (observed event rates / Standard Solar Model predictions) in Ga, Cl, and  $\nu e$  experiments, which are sensitive to lower, intermediate, and higher energy solar neutrinos, roughly speaking:

Ga:  $0.52 \pm 0.09$  (SAGE [8]),  $0.60 \pm 0.09$  (GALLEX [9])

Cl:  $0.32 \pm 0.03$  [4]

$\nu e$ :  $0.51 \pm 0.07$  [6]

In fact, in the present paper, we will explicitly demonstrate that, owing to the specific  $E_\nu$  dependence, there exists a rather broad range in  $(B, \Delta m^2)$  plane of band shape, which is an “allowed region” in order to reconcile all of the four

experimental data. (This possibility was explicitly pointed out in Ref. [16].) On the other hand, in MSW solution  $P_\nu$  approaches to 1, instead of 1/2, as  $E_\nu$  becomes very large. Thus to get a reasonably good fit to the observations in MSW,  $\theta$  (generation mixing angle) and  $\Delta m^2$  have to be carefully chosen [17]. This is the reason why in MSW there remain only two isolated rather restricted allowed regions in the  $(\theta, \Delta m^2)$  plane, though this restriction at the same time may enable us to pin down the correct set of parameters once the data get further improved.

After the results of Ga experiments were put forward, there have appeared some papers [18, 19], which also claim that RSFP scenario can reconcile the three kinds of experimental data. (As for the argument in the “hybrid”, MSW plus RSFP, scenario [20], see Ref [21]). In these papers the importance of the careful choice of the profile (position dependence) of the magnetic field  $B$  has been emphasized. Since our main point is to show that the all of the three deficit rates can be accounted for as a consequence of the desirable  $E_\nu$  dependence of  $P_\nu$  in RSFP, rather than the consequence of some special choices of  $B$  profile, we will be mainly concerned with the case with a constant  $B$  throughout the path of the solar neutrino propagation. Though the average deficit rates of three types of experiments are naturally reconciled for the constant  $B$  for rather broad range of the parameter space, we will further discuss how the allowed region is modified if  $B$  has different strengths in each of the convective ( $0.7 \leq r/r_\odot \leq 1.0$ ) and the inner zones ( $r/r_\odot < 0.7$ ) of the Sun. While our main focus is on the average deficit rates, we will also make some brief comments on the possible time variations of the event rates, since it was a original motivation of the OVV and RSFP scenarios.

Since our main purpose in the present paper is to clarify to what extent the specific features of RSFP, especially its desirable  $E_\nu$  dependence of the survival probability  $P_\nu$ , are useful in order to reconcile the three kinds of data, we consider pure RSFP of Majorana type in the 2 generation case,  $\nu_{eL} \rightarrow \bar{\nu}_{\mu R}$ , and neglect the generation mixing  $\theta$ . (We will not include the interesting effect [22, 23] due to the twisting of the magnetic field either.)

The time evolution of the system is governed by a Schrödinger-like equation [10];

$$i \frac{d}{dt} \begin{pmatrix} \nu_{eL} \\ \bar{\nu}_{\mu R} \end{pmatrix} = \begin{pmatrix} a_{\nu_e} & \mu B \\ \mu B & \frac{\Delta m^2}{2E_\nu} - a_{\nu_\mu} \end{pmatrix} \begin{pmatrix} \nu_{eL} \\ \bar{\nu}_{\mu R} \end{pmatrix}, \quad (1)$$

where  $\mu$  is the transition magnetic moment and the matter effects of neutrinos are given as  $a_{\nu_e} = \frac{G_F}{\sqrt{2}}(2N_e - N_n)$  and  $a_{\nu_\mu} = \frac{G_F}{\sqrt{2}}(-N_n)$ , with  $N_e$  and  $N_n$  being electron and neutron number densities. In getting predictions on the event rates in the three experiments we will numerically integrate the above equation, with the energy spectrum of each solar neutrino source and the absorption cross sections for Cl and Ga experiments being taken from Ref. [24]. As for the  $\nu_e$  experiment, the contribution from the  $\bar{\nu}_{\mu_R}e$  scattering is included together with the suitable trigger efficiency for the Kamiokande detector [5].

Before discussing the numerical results in detail, we will try to understand qualitatively how the  $E_\nu$  dependence shown in Fig. 1 naturally arises in RSFP. The argument goes as follows. For smaller  $E_\nu$  the level crossing between  $\nu_{e_L}$  and  $\bar{\nu}_{\mu_R}$  is not possible, and  $P_\nu \sim 1$ . For intermediate  $E_\nu$  the level crossing is realized and (as far as  $B$  is of suitable strengths) enough depletion of  $\nu_{e_L}$  becomes possible, i.e.  $P_\nu \sim 0$ . So far the behavior of  $P_\nu$  is similar to that in the MSW solution with relatively small  $\theta$ . An essential deviation from the MSW case becomes manifest when we consider the limit of large  $E_\nu$ . In the MSW, in this limit the transition  $\nu_{e_L} \rightarrow \nu_{\mu_L}$  tends to be non-adiabatic even though  $\nu_{e_L}$  experiences the level crossing, and  $P_\nu \rightarrow 1$ . Note that the adiabaticity condition in MSW,

$$\frac{\Delta m^2 \sin^2 2\theta}{E_\nu \cos 2\theta} \gg \frac{d(\ln N_e)}{dt} \quad (2)$$

is not satisfied for larger  $E_\nu$ . The situation is completely different in RSFP, since the  $E_\nu$  dependence of the argument of the Landau-Zener probability [25], a factor to judge the adiabaticity of the transition, is just opposite to the MSW case. Namely, the adiabaticity condition in RSFP,

$$\frac{(\mu B)^2 E_\nu}{\Delta m^2} \gg \frac{d(\ln N_e)}{dt}, \quad (3)$$

is well satisfied for large  $E_\nu$ . In Eq. (1) we realize that when  $E_\nu$  gets large the off-diagonal element  $\mu B$  in the  $2 \times 2$  ‘‘Hamiltonian’’ matrix becomes relatively important, and a ‘‘maximal mixing’’ between  $\nu_{e_L}$  and  $\bar{\nu}_{\mu_R}$  (corresponding to  $\theta \simeq \frac{\pi}{4}$  in the flavor mixing case) takes place. This is why  $P_\nu$  approaches to  $\frac{1}{2}$  in the large  $E_\nu$  limit, as is seen in Fig. 1.

Let us also point out a sort of scaling property. Fig. 2 shows profiles of  $P_\nu$  as a function of  $E_\nu/\Delta m^2$  for a few typical values of  $B$  with  $\mu = 10^{-11}\mu_B$ . From this figure we learn that when  $B$  scales as  $B \rightarrow \lambda B$ , approximately the same  $P_\nu$  is obtained once another parameter also scales as  $(E_\nu/\Delta m^2) \rightarrow (1/\lambda^2)(E_\nu/\Delta m^2)$ ,

for a suitable range of  $B$ . This means that almost the same  $P_\nu$  profile is obtained under the change of parameters,  $B \rightarrow \lambda B$  and  $\Delta m^2 \rightarrow \lambda^2 \Delta m^2$ . It is interesting to note that this scaling leaves the argument of the Landau-Zener probability,  $(\mu B)^2 E_\nu / (\Delta m^2 (d \ln N_e / dt))$ , unchanged. Thus  $P_\nu$  is roughly controlled by the adiabaticity of the transition.

What the scaling property suggests is that the allowed region in the  $(B, \Delta m^2)$  plane is roughly along a line  $\Delta m^2 / B^2 \simeq \text{constant}$ , as has been confirmed by the explicit numerical calculations of the allowed range, shown in Fig. 3 (assuming  $\mu = 10^{-11} \mu_B$ ). Fig. 3 presents our numerical results of the allowed regions, in order to account for four experiments simultaneously at 99%, 95%, and 90% confidence levels. Though the allowed regions in Fig. 3 are rather broad, too small or too large magnetic field  $B$  is not favored. The reason is that too small  $B$  makes the transition non-adiabatic, and too large  $B$  leads to a uniform depletion of solar neutrinos by a factor 1/2 (though the contribution from the  $\bar{\nu}_{\mu_R} e$  scattering causes a little bit higher event rate in Kamiokande). Thus the allowed region of the parameters are (at 99% C.L.),

$$25 \leq B \leq 130 \text{ (kG) ,}$$

$$7 \times 10^{-9} \leq \Delta m^2 \leq 2 \times 10^{-7} \text{ (eV}^2\text{)}.$$

In the above discussions we assumed a uniform magnetic field  $B$ , though it is most probably unrealistic. The reason was twofold. First, our knowledge of the magnetic field profile, especially in the inner zone, is very poor. Secondly, we aimed to extract as much as possible the genuine feature of RSFP, irrespectively of specific choices of  $B$  profile, although the specific choices of  $B$  have been discussed to be helpful in reconciling the three solar neutrino data in the literature [18, 19]. When we consider the possible time-dependence of the event rates, however, the assumption of time dependent but uniform  $B$  may be too simple-minded and may lead to a “really” unrealistic consequence. This is because the  $pp$  neutrinos detected in Ga experiment with relatively lower energies experience the level crossing at the inner zone for the values of  $\Delta m^2$  inside the allowed region of Fig. 3, while the crossing points of  $^8\text{B}$  and  $^7\text{Be}$  neutrinos are mostly in the convective zone. We should note that it is, at least, a general consensus that the magnetic field  $B$  varies periodically only in the convective zone, and the strengths of  $B$  in the two zones can be quite different, in general.

We therefore will finally analyze in some detail the consequences of taking different magnitudes of magnetic fields in convective and inner zones, denoted by  $B_c$  and  $B_i$ , respectively. Only two extreme cases are considered here as the

choices of  $B_i$ , i.e., (a)  $B_i = 0$ , and (b)  $B_i = 10^3$  (kG). In these two typical cases the  $E_\nu/\Delta m^2$  dependence of  $P_\nu$  have been shown in Fig. 4, for several values of  $B_c$ . Fig. 4 clearly shows that the lower energy part is greatly affected by the choice of  $B_i$ , since the level crossings of the lower energy neutrinos happen in the inner zone; when  $B_i = 0$  (case (a)), the lower energy part has almost no depletion, while when  $B_i = 10^3$  (kG) (case (b)), the lower energy part gets strong suppressions. We have again calculated the allowed regions in  $(B_c, \Delta m^2)$  plane to reconcile all solar neutrino data at 95% C.L. for cases (a) and (b), whose results have been demonstrated in Fig. 5. (The region (c) is for the case  $B_i = B_c$ , and has already appeared in Fig. 3, but has been included for the sake of comparison.) As is seen in this figure, in the case (a) there scarcely remains the allowed region only when  $B$  is rather strong. This is because the neutrino oscillation is possible only in the convective zone ( $B_i = 0$ ), and when  $B$  is strong we cannot expect the  $E_\nu$  dependence of the survival probability, just as in the OVV scenario. In the figure in case (b) very small  $\Delta m^2$  is favored. This is because unless  $\Delta m^2$  is very small lower energy neutrinos, detectable at the Ga experiment, suffer from too strong depletion, as is clear in Fig. 4 for case (b), which contradicts with the data. Though all of three cases have their own allowed regions, each case has different  $\chi^2$  minimum:  $\chi_{min}^2 = 2.0, 3.8$  and  $3.0$  for 2 degrees of freedom (4 data – 2 parameters) for cases (a), (b), and (c), respectively. Thus the case (b) may not be preferred as a possible solution, and the case (c) seems to be the most reasonable solution.

How about the time variations of the event rates? Instead of considering the time variations themselves we will discuss the variations of the solar neutrino event rates as the functions of the convective zone magnetic field  $B_c$ . Though the average event rates can be most reasonably explained in case (c), the assumed relation  $B_i = B_c$  should be understood to hold only in average, and  $B_c$  should be regarded to modulate around the average value. We therefore choose  $B_i$  to be the central values of  $B$  in the allowed region of Fig. 3 (or in Fig. 5 for case (c)) for a few representative values of  $\Delta m^2$  in the allowed region, i.e.  $B_i = 30, 60$ , and  $90$  (kG) for  $\Delta m^2 = 10^{-8}, 4 \times 10^{-8}$ , and  $10^{-7}$  (eV<sup>2</sup>), respectively, and the variations of the event rates have been plotted as the functions of  $B_c$  in Fig. 6 for these choices of  $B_i$  and  $\Delta m^2$ . In Fig. 6, it is hard to find out a reasonable parameter choice, which clearly shows the claimed time dependence of the data. We have also calculated the variations for other cases (b) and (c) as well, but no better result has been obtained.

As a summary, we have argued and have shown by explicit numerical calcu-

lations that all three types of solar neutrino experimental data on their capture rates can be naturally reconciled by the Resonant Spin-Flavor Precession (RSFP) scenario. This is mainly because the  $E_\nu$  (neutrino energy) dependence of the  $\nu_e$  survival probability  $P_\nu$ , specific in RSFP, is suitable for reconciling the data. Because of this property, there appears a rather broad allowed region in the  $(B, \Delta m^2)$  plane ( $B$ : strength of magnetic field), which provides a reasonably good fit to the three experimental data. The good fit is available even for a simple-minded assumption of a uniform  $B$ . We have, in addition, analyzed the consequences of taking different  $B$ 's in convective and inner zones:  $B_c, B_i$  respectively. We have found that if  $B_i$  is very weak a there scarcely remains the allowed region, while too strong  $B_i$  seems to be not preferred. As for the time variations of the event rates of three types of experiments, to get reasonable behaviors seems to be non-trivial, and in our rather restricted choice of parameter set we have not succeeded in it. Of course, various additional possibilities will be opened if we adopt more elaborate  $B$  profiles [18, 19], or if we include a generation mixing in addition to RSFP (see Ref. [21]).

## References

- [1] S. P. Mikheyev and A. Yu. Smirnov, Sov. J. Nucl. Phys.**42**, 913 (1985); L. Wolfenstein, Phys. Rev. **D17**, 2369 (1978).
- [2] L. B. Okun, M. B. Voloshin, and M. I. Vysotsky, Sov. Phys. JETP **64**, 446 (1986).
- [3] R. Davis Jr., Proc. Int. Symp. on Neutrino Astrophysics “*Frontiers of Neutrino Astrophysics*”, ed. by Y. Suzuki and K. Nakamura, Universal Acad. Press, Tokyo, p. 47 (1993).
- [4] K. Lande, in *Neutrino 94*, Israel, June, 1994.
- [5] K. S. Hirata *et al.*, Phys. Rev. Lett. **65** 1297 (1990); **65**, 1301 (1990); **66**, 9 (1991); Phys. Rev. **D 44**, 2241 (1991).
- [6] Y. Suzuki, in *Neutrino 94*, Israel, June, 1994.
- [7] SAGE Collaboration, A. I. Abazov *et al.*, Phys. Rev. Lett. **67**, 3332 (1991); SAGE Collaboration, J. N. Abdurashitov *et al.*, Phys. Lett. **B 328**, 234 (1994).
- [8] J. Nico, in *27th ICHEP*, United Kingdom, July, 1994.



- [9] GALLEX Collaboration, P. Anselmann *et al.*, Phys. Lett. **B285**, 376 (1992); **B285**, 390 (1992); **B327**, 377 (1994).
- [10] C. S. Lim and W. J. Marciano, Phys. Rev. **37**, 1368 (1988).
- [11] E. Kh. Akhmedov, Sov. J. Nucl. Phys. **48**, 382 (1988); Phys. Lett. **B213**, 64 (1988).
- [12] C. S. Lim, M. Mori, Y. Oyama, and A. Suzuki, Phys. Lett. **B243**, 389 (1990).
- [13] R. Barbieri and R. N. Mohapatra, Phys. Rev. Lett. **61**, 27 (1988); J. M. Lattimer and J. Cooperstein, Phys. Rev. Lett. **61**, 23 (1988).
- [14] M. Fukugita and S. Yazaki, Phys. Rev. **D36**, 3817 (1987).
- [15] K. S. Babu, R. N. Mohapatra, and I. Z. Rothstein, Phys. Rev. **D44**, 2265 (1991); Y. Ono and D. Suematsu, DPKU9206, BUTP-92/09 (1992); E. Gates, L. Krauss and M. White, Phys. Rev. **D46**, 1263 (1992).
- [16] C.S. Lim, Proceedings of Int. Symp. on Neutrino Astrophysics “*Frontiers of Neutrino Astrophysics*”, ed. by Y. Suzuki and K. Nakamura, Universal Acad. Press, Tokyo, p117 (1993).
- [17] N. Hata and P. Langacker, Phys. Rev. **D50**, 632 (1994).
- [18] E. Kh. Akhmedov, A. Lanza, and S. T. Petcov, Phys. Lett. **B303**, 85 (1993).
- [19] J. Plido, Phys. Rev. **D48**, 1492 (1993).
- [20] H. Minakata and H. Nunokawa, Phys. Rev. Lett. **63**, 121 (1989); A. B. Balantekin, P. J. Hatchell and F. Loreti, Phys. Rev. **D41**, 3583 (1990).
- [21] H. Nunokawa and H. Minakata, Phys. Lett. **B314**, 371 (1993).
- [22] J. Vidal and J. Wudka, Phys. Lett. **B249**, (1990) 473; E. Kh. Akhmedov, P. I. Krastev, and A. Yu. Smirnov, Z. Phys. **C52**, 701 (1991); T. Kubota, T. Kurimoto, M. Ogura, and E. Takasugi, Phys. Lett. **B292**, 195 (1992); C. Aneziris and J. Schechter, Phys. Rev. **D45**, 1053 (1992); A. B. Balantekin and F. Loreti, Phys. Rev. **D45**, 1059 (1992).
- [23] P. I. Krastev, Phys. Lett. **B303**, 75 (1993).
- [24] J. Bahcall and R. Ulrich, Rev. of Mod. Phys. **60**, 297 (1988); J. N. Bahcall, *Neutrino Astrophysics*, Cambridge University Press, New York, (1989).

[25] S. J. Parke, Phys. Rev. Lett. **57**, 1275 (1986).

## Figure Captions

Fig. 1: The conceptualized  $E_\nu/\Delta m^2$  dependence of the  $\nu_e$  survival probability  $P(\nu_e \rightarrow \nu_e)$  in RSFP

Fig. 2: The profiles of  $P_\nu$  as the functions of  $E_\nu/\Delta m^2$  for  $B = 10, 30, 50$  and  $100$  kG respectively with  $\mu = 10^{-11}\mu_B$  assumed.

Fig. 3: The allowed regions to account for the data of the three types solar neutrino experiments simultaneously, at 99, 95, and 90% C.L.

Fig. 4: The  $E_\nu/\Delta m^2$  dependence of  $P_\nu$  for two different choices of the inner zone magnetic field  $B_i$ , i.e. (a)  $B_i = 0$ , and (b)  $B_i = 10^3$  (kG), each for  $B_c = 10, 30, 50$ , and  $100$  kG.

Fig. 5: The allowed regions in  $(B_c, \Delta m^2)$  plane (95% C.L.), similar to Fig. 3, but now assuming two typical cases for the strength of  $B_i$ , i.e.  $B_i = 0$  (region (a), disconnected 5 black areas) and  $B_i = 10^3$  kG (region (b)). The region (c) is the same as in Fig. 3 but has been included for comparison.

Fig. 6: The variations of event rates of three types of experiments as the functions of  $B_c$  for three choices of remaining parameters, i.e. (i)  $B_i = 30$  (kG),  $\Delta m^2 = 10^{-8}$  (eV<sup>2</sup>), (ii)  $B_i = 60$  (kG),  $\Delta m^2 = 4 \times 10^{-8}$  (eV<sup>2</sup>), and (iii)  $B_i = 90$  (kG),  $\Delta m^2 = 10^{-7}$  (eV<sup>2</sup>).

This figure "fig1-1.png" is available in "png" format from:

<http://arxiv.org/ps/hep-ph/9410389v2>

This figure "fig1-2.png" is available in "png" format from:

<http://arxiv.org/ps/hep-ph/9410389v2>

This figure "fig1-3.png" is available in "png" format from:

<http://arxiv.org/ps/hep-ph/9410389v2>

This figure "fig1-4.png" is available in "png" format from:

<http://arxiv.org/ps/hep-ph/9410389v2>

This figure "fig1-5.png" is available in "png" format from:

<http://arxiv.org/ps/hep-ph/9410389v2>

This figure "fig1-6.png" is available in "png" format from:

<http://arxiv.org/ps/hep-ph/9410389v2>



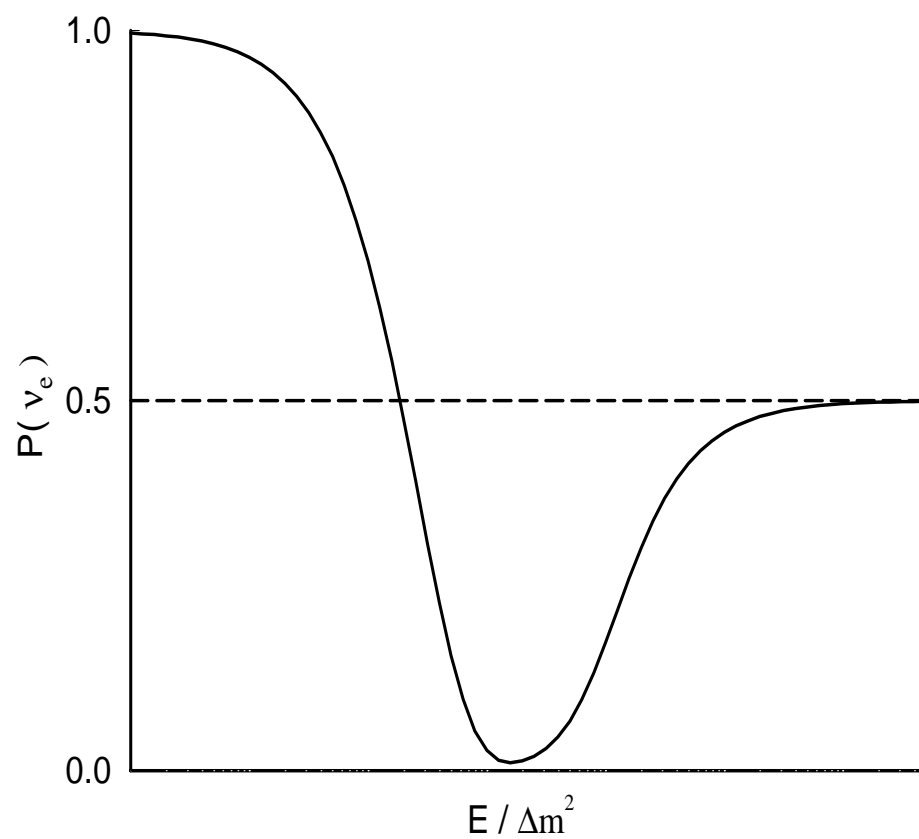


**Fig. 1**

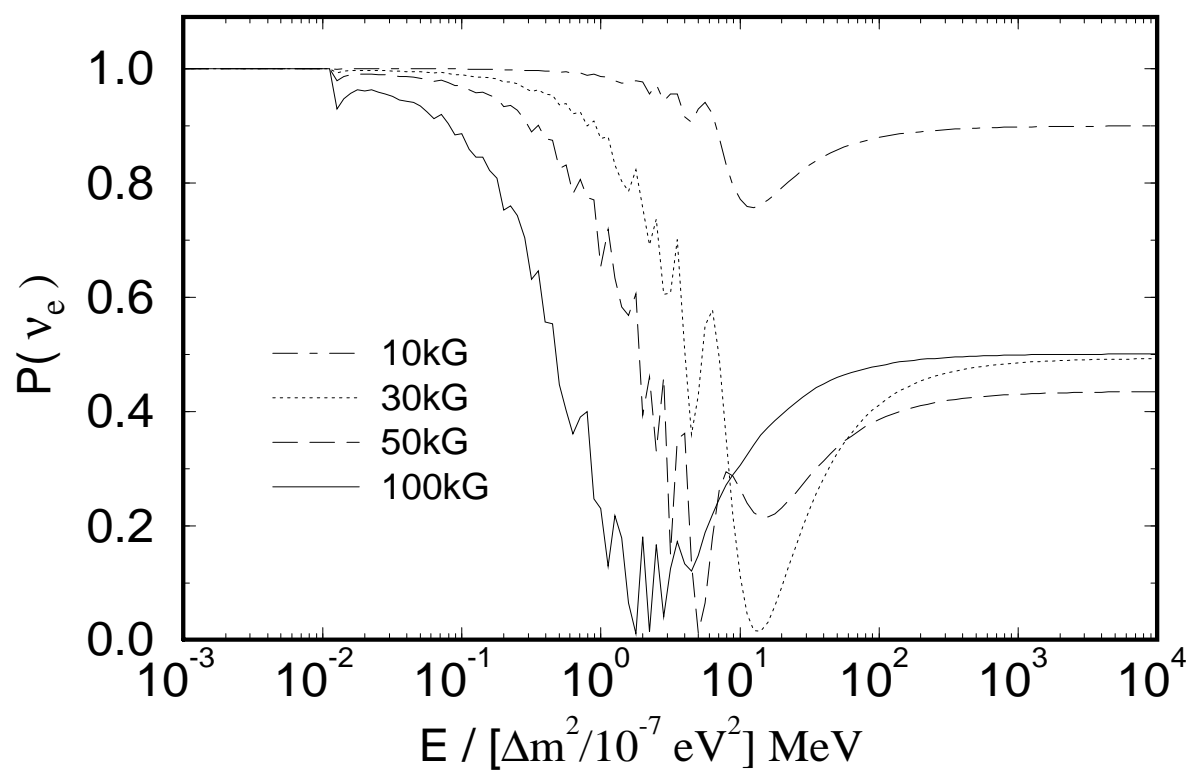


**Fig. 2**

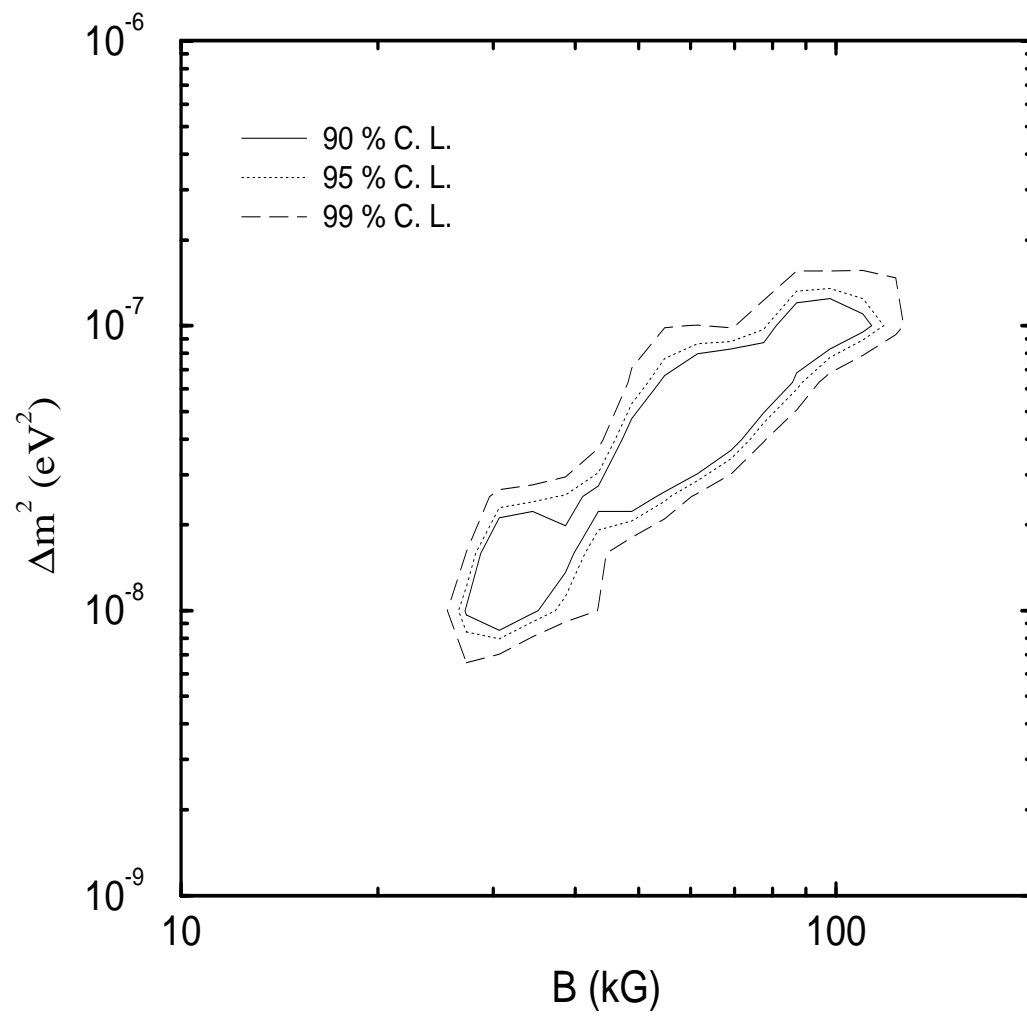


**Fig. 3**

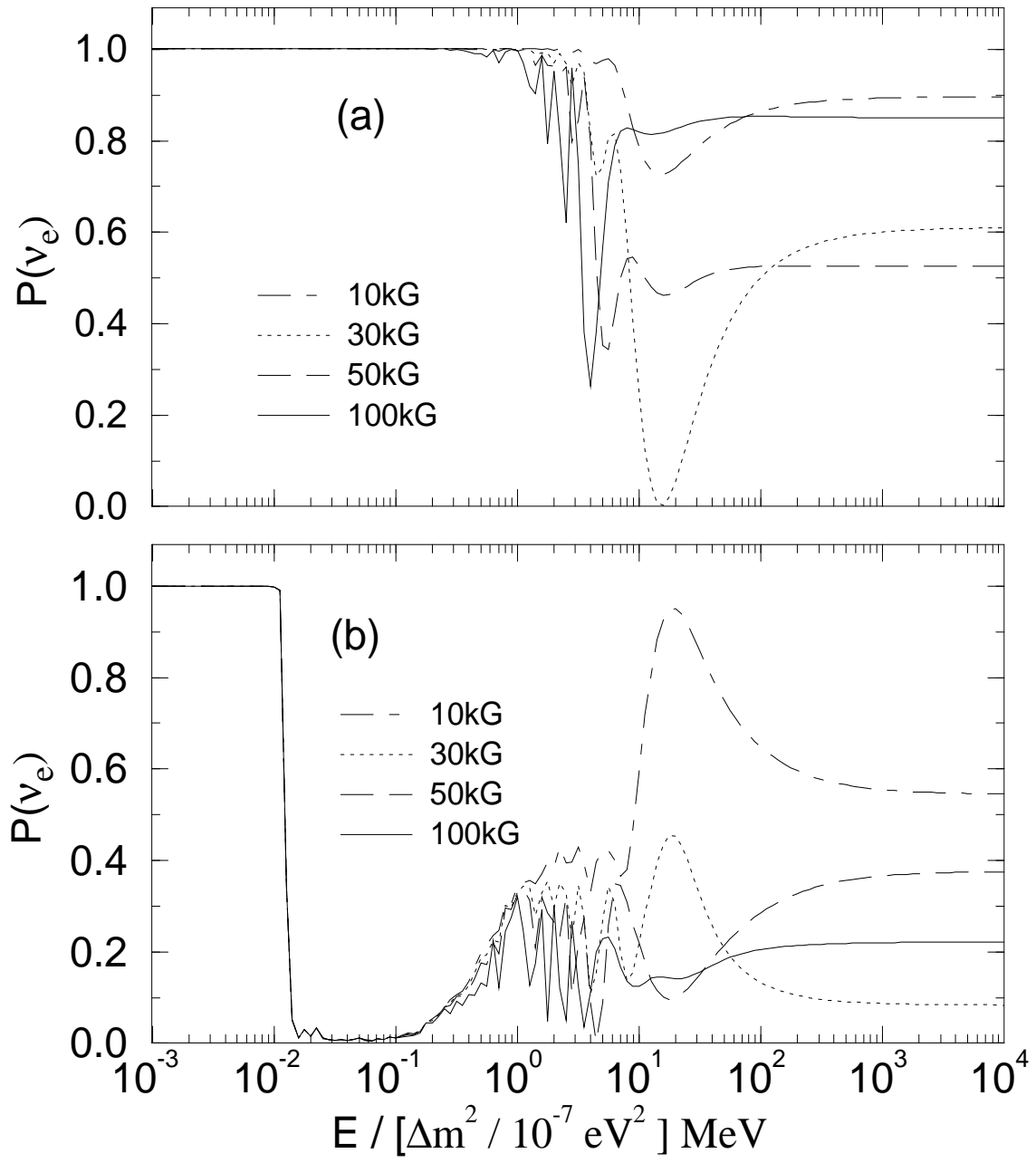


**Fig. 4**

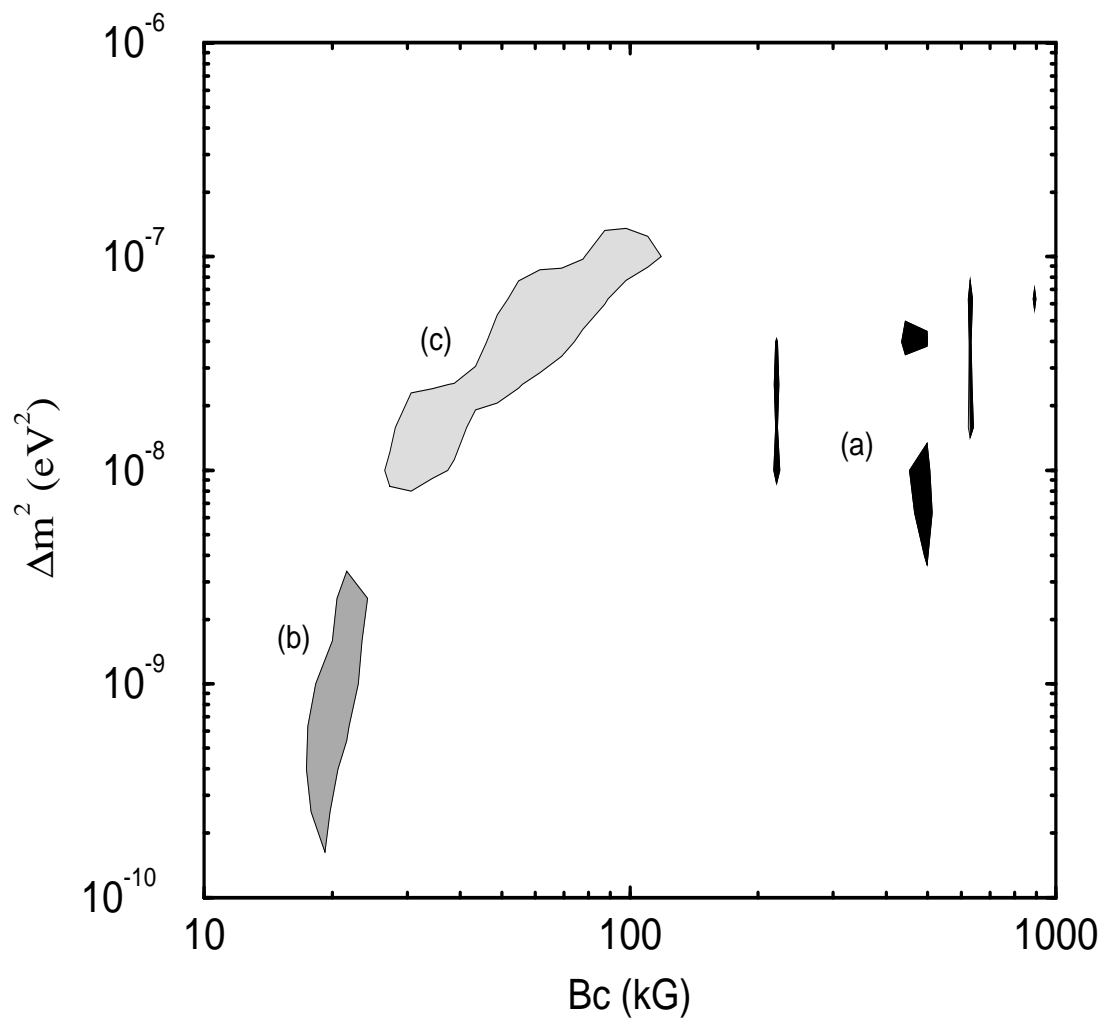


**Fig. 5**

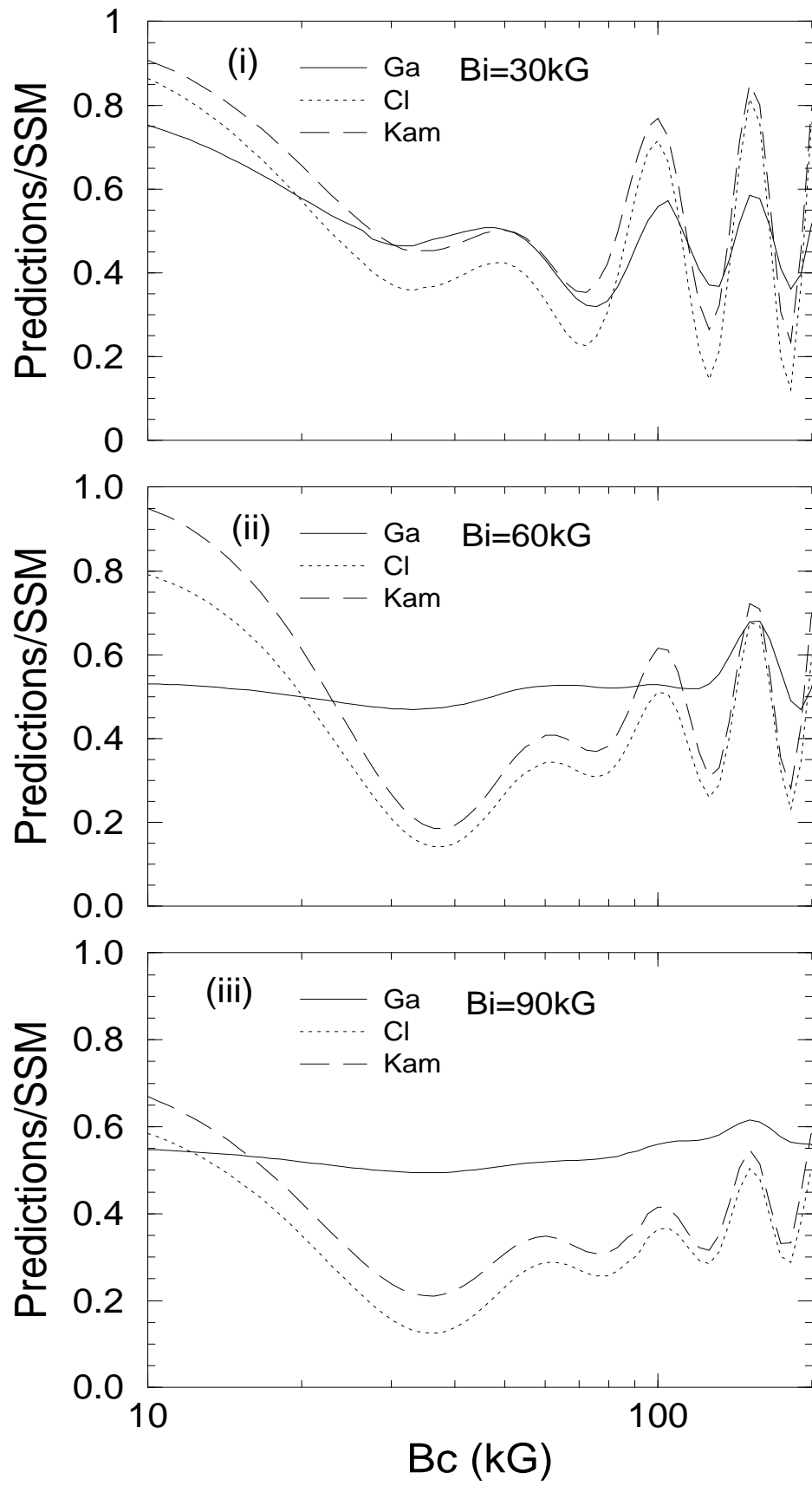


**Fig. 6**